Spatial heterogeneity of natural and socio-economic features shape that of ecosystem services. A large-scale study on the Yangtze River economic Belt, China

Zeyang Xie, Liujie He, Zhun Mao, Wei Wan, Xu Song, Zhijian Wu, Han Liang, Jing Liu, Bofu Zheng, Jinqi Zhu

Ecological Indicators 159 (2024) 111729

Contents lists available at ScienceDirect

Ecological Indicators

journal homepage: www.elsevier.com/locate/ecolind

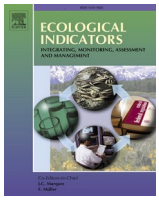

Original Articles

Spatial heterogeneity of natural and socio-economic features shape that of ecosystem services. A large-scale study on the Yangtze River economic Belt, China

Zeyang Xie [a,b], Liujie He [a], Zhun Mao [c], Wei Wan [a,b], Xu Song [a], Zhijian Wu [a], Han Liang [a], Jing Liu [a], Bofu Zheng [a,b,*], Jinqi Zhu [a,b,*]

[a] School of Resources and Environment, Jiangxi Institute of Ecological Civilization, Nanchang University, Nanchang 330031, China
[b] Engineering Research Center of Watershed Carbon Neutralization, Ministry of Education, Nanchang University, Nanchang 330031, China
[c] Univ Montpellier, AMAP, INRAE, CIRAD, CNRS, IRD, 34000 Montpellier, France

ARTICLE INFO

Keywords:
Ecosystem services
Multiscale geographic weighted regression
Threshold analysis
Yangtze river economic belt

ABSTRACT

Investigating large-scale spatial patterns of ecosystem services (ESs) and their underlying drivers can greatly contribute to policies-making and regional sustainability development. With water yield (WY), soil conservation (SC), and carbon sequestration (CS) as representative ESs, we aim to quantify their spatial patterns in the Yangtze River Economic Belt, China, and to identify their driving factors, and to formulate sound environmental management strategies. Spatial geography and socioeconomic data from 2000 to 2020 were mined and a range of research methods, including multiscale geographic weighted regression, self-organizing maps, and linear discriminant analysis, were employed for such a purpose. Annual average WY, SC, and CS were 403 mm, 9897 $t{\cdot}km^{-1}$, and 1071 $g{\cdot}CO_2{\cdot}m^{-2}$. The three ESs examined exhibit spatial heterogeneity. WY exhibited significant patterns of variation along the north–south gradient, while SC and CS exhibited significant variation along the topographic gradient. In the context of high correlation of driving factors among ESs, WY and SC exhibited a greater sensitivity to natural factors (such as precipitation), while CS demonstrated a height sensitivity to human activities in addition to vegetation cover. Spatial heterogeneity is pronounced among the main driving factors of ESs. Three threshold equations were established to describe the manner in which driving factors of different regional ecosystem services undergo transformations, equations possessed a high level of credibility in this study (coincidence $>$ 80 %). This study reveals spatial variations in ecosystem services and their natural and socio-economic drivers. More specifically, we quantitatively validated the threshold in the expression of ecosystem service drivers, establishing a strong scientific foundation for regional ecosystem conservation and management.

1. Introduction

Ecosystem services (ESs), play an important role in the survival and development of humankind (Comberti et al., 2015). Thus, humans need to pay sufficient attention to the maintaining ESs in their decision-making for sustainable development (Costanza et al., 1997).

Studying the spatial patterns of ESs is of great importance in balancing regional economic development and environmental protection (Gret-Regamey et al., 2017). At present, ESs are often characterized using the spatial mapping of ESs across different gradients (Yang et al., 2020). Some studies have explored the spatial distribution of ESs across gradients of altitude (Gomes et al., 2020), terrain (Wu et al., 2022a), land-sea (Liu et al., 2020), and aridity (Garcia-Palacios et al., 2018). However, most studies focus on a single gradient, which is usually a natural one. Few studies have considered ES changes over multiple gradients (Ma et al., 2021). Compared to natural gradients, socio-economic gradients have received less attention, although they are sometimes considered in several studies on ES changes along an urban–rural gradient (Gonzalez-Garcia et al., 2020; Kroll et al., 2012). These studies revealed a significant impact of human activities on ESs. Therefore, all these results suggest the importance of incorporating a multitude of gradients ranging from natural to social-economic ones for a better understanding of the spatial distribution of ESs.

Identifying driving forces of ESs are a central issue in ESs research

* Corresponding authors at: School of Resources and Environment, Jiangxi Institute of Ecological Civilization, Nanchang University, Nanchang 330031, China.
E-mail addresses: bfzhen@ncu.edu.cn (B. Zheng), Zhujq@ncu.edu.cn (J. Zhu).

https://doi.org/10.1016/j.ecolind.2024.111729
Received 4 November 2023; Received in revised form 28 January 2024; Accepted 8 February 2024
Available online 17 February 2024

and a prerequisite for their sustainable use (Hernandez-Blanco et al., 2022). Existing studies have found that land use and land cover change (LUCC) (Song and Deng, 2017), climate (Berdugo et al., 2020), topography (Ma et al., 2021; Zhang et al., 2022; Zhang and Hu, 2021), and policies (Bai et al., 2016; Bardgett et al., 2021; Tang et al., 2022; Tedesco et al., 2023), could profoundly modify regional ES patterns. Moreover, these drivers themselves can equally show complex spatial patterns (Fu et al., 2013; Zhao et al., 2023). (He et al., 2019). Accordingly, the spatial heterogeneity of ESs can be the consequence of the combined effects of multiple drivers in space. Therefore, it is of great meaningfulness to quantify the spatial patterns of both ESs and potential drivers and then to have them coupled. Yet, so far, many studies studying the relationship between ESs and drivers did not adequately consider spatial patterns of ES drivers. To explore ES drivers, these studies rely on diverse approaches, including correlation coefficients (Hu et al., 2023; Rötzer et al., 2019), the coefficient of sensitivity (Kreuter et al., 2001; Sanchez-Canales et al., 2012), variance (Lin and Yun, 2023; Xiao and Ouyang, 2019; Zhang et al., 2018), and Ordinary Least Squares (OLS) (Chen et al., 2022; Liu et al., 2021). Although these approaches are simple and easy to implement, they present technical difficulties when it comes to taking into account the spatial heterogeneity of ES factors.

To consider the spatial patterns of the ES drivers, more sophisticated modelling approaches have been elaborated as alternatives, such as Geographically Weighted Regressions (GWR) (Ahmed et al., 2017; Sun et al., 2020; Yang et al., 2021), a Geodetector (Hu et al., 2021; Hu et al., 2022a; Li et al., 2022a), and a Multiscale Geographic Weighted Regression (MGWR) (Liu et al., 2022). Compared with those simple approaches, e.g., OLS or GWR, MGWR offers greater explanatory power and a higher goodness of fit (Pang et al., 2022; Xue et al., 2023). In these more sophisticated approaches, spatially heterogeneous ES drivers can originate from different pools of factors which can be either natural or social-economic ones. However, few studies have used these latter methods to elucidate large-scale spatial patterns of ESs with spatially complex drivers.

The Yangtze River Economic Belt (YEB) (The State Council Information Office of the People's Republic of China, 2020), a region that comprehensively considers the administrative units of the Yangtze River Basin and a compound area composed of natural geography and economic social spaces (Li et al., 2022b; Zhao and Zhao, 2023). The YEB is one of China's regions with the highest economic, population, and human activities. There are imbalances in the ecological environment (Bao et al., 2020; Tan et al., 2023), economic development (Wang et al., 2022a; Xiang et al., 2019), industrial layouts (Tang et al., 2019; Yuan et al., 2022), and coupling between various elements (Li et al., 2022c). The YEB spans approximately 10 latitudes and includes both subtropical and temperate climates, with elevations ranging from 0 to 5500 m. At the same time, WY, SC, and CS form the foundation for regional development and are generally believed to benefit around 400 million people. In 2020, WY alone provided the region with 2645.1 billion m^3 of water resources (Liu et al., 2022a). SC contributes around 34.67 million hectares of healthy arable land (Abdul-Rahim et al., 2018), and the region's potential for CS is expected to be substantial due to its favorable vegetation coverage (Tian et al., 2022). Thus, the ESs value of this region accounts for 45.77 % of that of the country (Xie et al., 2015). Yet, due to the complexity of the region itself and diversity of methods, diagnoses on ES drivers of the YEB are usually inconsistent among studies. For example, water yield (WY) indicated precipitation as the main driver (Wang et al., 2022d), while others suggested this to be the Digital Elevation Model (DEM) (Wang et al., 2023); the effect of temperature on WY was found to be both negative (Wei et al., 2022) and positive (Yin et al., 2020). It is therefore necessary to enrich the evidence and validate these diagnoses by carrying out additional studies.

In this study, YEB is selected as our case study with a county-level resolution for the quantification of ESs and factors as potential ES drivers. We aim to: (1) quantify the spatial distribution of ESs (WY, SC, CS) from 2000 to 2020 and assess their spatial heterogeneity across five gradients (in terms of both natural and socio-economic aspects). (2) explore the main drivers of the ESs by quantifying the patterns of different factors and having them coupled with ES patterns; and (3) clarify the sensitivity of the ESs to different drivers and find the threshold for the transformation of the main driving factors. As such, this research contributes to the study of spatial heterogeneity and variation characteristics of ESs at different scales in the YEB, as well as the establishment of the links between multiple driving factors, which ultimately helps us to develop a more scientific and reasonable ecological protection strategy system for the YEB.

2. Methods and materials

2.1. Study area

The YEB uses water as a carrier and link, connecting the upper, middle, and lower reaches; the eastern, middle, and western regions; the left and right banks; and the main tributaries, forming a holistic and open natural ecosystem. The YEB has a wide range, with an area of approximately 2.05×10^6 km^2, located between 21°8′–35°1′N and 97°3′–121°6′E (Fig. 1). Natural and geographic conditions differ from province to province. Mean annual precipitation is high in the west and low in the east, with approximately 1000–1600 mm. Altitude gradually decreases from the coast to the interior, and the difference is relatively large (4–2000 m). The proportion of forest gradually decreases from south to north, from 55 % to 11 %.

The YEB is one of three major national strategic development areas in China and an inland river economic belt with global influence that includes 11 provinces and cities and more than 1,000 counties and cities. In 2020, the gross domestic product (GDP) of this region reached 47.1 trillion CNY and its population reached 790 million people, accounting for 46.4 % and 56.5 % of the country, respectively. There are 60 cities with populations of more than one million people in the YEB. Policies focus on crossing administrative regions and coordinating regional development. However, huge differences can be found throughout the YEB in terms of development of resources, environment, transport, and industrial bases. According to statistics for the upper, middle, and lower reaches, GDP per capita in the middle and upper regions is only 60.3 % and 49.2 % that of the lower regions. The gap among the levels of basic public service in regions is pronounced.

2.2. Data sources

The main data used in this study included land use and land cover (LULC), DEM, the Normalized difference vegetation index (NDVI), net primary productivity (NPP), precipitation (Pre), temperature (Tem), evapotranspiration, soil properties, and socio-economic data. The data sources are summarized in Table 1. Prior to analysis, all data were resampled into a 1 km resolution raster dataset.

2.3. Ecosystem service evaluation

Three main ESs were selected, namely the WY, SC, and CS, and corresponding models were used to quantify them. The study years were 2000, 2005, 2010, 2015, and 2020. The grid scale in the calculation process was 1 km, and the calculation results were counted for each counties of the YEB.

WY refers to the capacity of annual water supply for industrial production, agricultural activities, and human consumption. In this study, the Annual Water Yield model in InVEST (version 3.11.0, USA) was used to quantify the WY supply, expressed as Eqs. (1)–(5):

$$Y_{xi} = \left(1 - \frac{\mathrm{AET}_{xi}}{P_x}\right) \times P_x \quad (1)$$

where Y_{xi} represents the annual water yield in mm for pixel x in an area

Fig. 1. Location of the study area.

with a LULC classification *i*; AET_{xi} represents the actual evapotranspiration in mm for pixel *x* in an area with LULC classification *i*; P_x represents the annual precipitation in mm for pixel *x* (Table 1).

$$\frac{\mathrm{AET}_{xi}}{P_x} = 1 + \frac{\mathrm{PET}_{xi}}{P_x} - \left[1 + \left(\frac{\mathrm{AET}_{xi}}{P_x}\right)^{\omega}\right]^{1/\omega} \tag{2}$$

where $\frac{\mathrm{AET}_{xi}}{P_x}$ reflects the dimensionless water balance (Zhang et al., 2001); PET_{xi} is potential evapotranspiration for pixel *x* in an area with LULC classification *i*; ω is a nonphysical empirical fitting parameter that characterizes the land surface properties of catchments, dimensionless, estimated following the approach proposed by (Donohue et al., 2012) as in Eq. (3):

$$\omega = Z\frac{AWC}{P} + 1.25 \tag{3}$$

where *AWC* is the volumetric (mm) plant available water content calculated using Eq. (4); *Z* is an empirical constant with a value of 15.

$$AWC = \mathrm{Min}(\ layerdepth,\ rootdepth\ ) \cdot PAWC \tag{4}$$

where *layerdepth* is the soil depth at which root penetration is inhibited, estimated using soil depth; *rootdepth* is often given as the depth at which 95 % of a vegetation type's root biomass occurs, estimated using soil depth (Table 1); *PAWC* is the plant available water capacity, dimensionless, calculate using Eq. (5):

Table 1
Data descriptions and sources.

Data	Description	Data source
LULC	Land use and land cover in 2000, 2005, 2010, 2015, and 2020 with a 30 m spatial resolution	Resources and Environment Sciences (https://www.resdc.cn)
DEM	The digital elevation model with a 150 m spatial resolution	Resources and Environment Sciences (https://www.resdc.cn)
NDVI	Annual NDVI from 2000 to 2020 with a 1000 m spatial resolution	Resources and Environment Sciences (https://www.resdc.cn)
NPP	NPP from 2000 to 2020 with a 1000 m spatial resolution	Resources and Environment Sciences (https://www.resdc.cn)
Precipitation Temperature Evapotranspiration	The multi-year average value obtained by interpolating the data of each site	The China Meteorological Data Service Center (https://data.cma.cn)
Soil property data	Soil depth and the content of sand, silt, clay, and organic carbon.	Food and Agriculture Organization (FAO)
Socio economic	GDP, population, industrial output value from 2000 to 2020	China County Statistical Yearbook and Local statistical yearbooks of YEB (https://data.cnki.net)

$$PAWC = 54.509 - 0.132\ m_s - 0.03(m_s)^2 - 0.55\ m_{silt} - 0.006(m_{silt})^2 - 0.738\ m_c + 0.007(m_c)^2 - 2.688 orgC + 0.501(orgC)^2 \quad (5)$$

where m_c represents the percentage (%) of clay particles (<0.002 mm); m_{silt} represents the percentage of silt particles (0.002–0.05 mm); m_s represents the percentage of sand particles (0.05–2 mm); *orgC* represents the percentage of organic carbon in the soil. All were estimated using soil property data (Table 1).

SC was quantified using the RUSLE model in InVEST, expressed as Eqs. (6)–(9):

$$SC_x = R_x \times K_x \times L_x \times S_x \times (1 - C_x \times P_x) \quad (6)$$

where SC_x represents the soil conservation on pixel x per year, t·a^{-1}; R_x is the rainfall erosivity factor, dimensionless, on pixel x; K_x is the soil erodibility factor, dimensionless, on pixel x; L_x is the slope length factor, dimensionless, on pixel x; S_x is the slope steepness factor, dimensionless, on pixel x; C_x is the cover management factor on pixel x, dimensionless, dependent on the LULC, referencing multiple studies (Kong et al., 2018; Rao et al., 2016); P_i represents the factor for conservation practices, dependent on LULC, referencing multiple studies (Xu et al., 2018).

Calculation R refers to the work of Zhang et al. (Zhang et al., 2002), expressed as Eqs. (7)–(8):

$$R = \sum_{j=1}^{24} M_j \quad (7)$$

$$M = \alpha \sum_{d=1}^{K} P_i^{\beta} \quad (8)$$

where M is the half monthly rainfall erosivity, mm·hm^{-2}·h^{-1}·a^{-1}; P_i represents the erosive rainfall within half a month (rainfall ≥ 12 mm, otherwise considered as 0) in mm, estimated using daily rainfall data (Table 1); j represents the half months per year, with values of 24, dimensionless; d represents the days of a half month; K depends on the number of days, dimensionless; α and β are coefficients taken from other studies (Sun et al., 2011), with values of 0.39 and 1.72, dimensionless.

Calculation K refers to the work of (Williams et al., 1989), expressed as Eq. (9):

$$K = \{0.2 + 0.3exp\ [-0.0256 m_s \times (1 - m_{slit})\ ]\} \times [m_{slit}/(m_c + m_{slit})]^{0.3} \times \{1 - 0.25 orgC/[orgC + \exp(3.72 - 2.85 orgC)]\} \times \{1 - 0.7(1 - m_s/100)/\{(1 - m_s/100) + exp[-5.51 + 22.9(1 - m_s/100)]\}\} \quad (9)$$

where m_c represents the percentage (%) of clay particles (<0.002 mm); m_{silt} represents the percentage of silt particles (0.002–0.05 mm); m_s represents the percentage of sand particles (0.05–2 mm); *orgC* represents the percentage of organic carbon in the soil estimated using soil property data (Table 1).

L and S were calculated using Eqs. (10)–(12):

$$S = \begin{cases} 10.8\sin\theta + 0.03 & \theta \leqslant 5^{\circ} \\ 16.8\sin\theta - 0.50 & 5^{\circ} < \theta \leqslant 10^{\circ} \\ 20.204\sin\theta - 1.2404 & 10^{\circ} < \theta \leqslant 25^{\circ} \\ 29.585\sin\theta - 5.6079 & \theta > 25^{\circ} \end{cases} \quad (10)$$

$$L = \left(\frac{\lambda}{22.13}\right)^{m} \quad (11)$$

$$m = \begin{cases} 0.2 & \theta \leqslant 1^{\circ} \\ 0.3 & 1^{\circ} < \theta \leqslant 3^{\circ} \\ 0.4 & 3^{\circ} < \theta \leqslant 5^{\circ} \\ 0.5 & \theta > 5^{\circ} \end{cases} \quad (12)$$

where θ is the slope angle, λ is the horizontal distance of the slope length (m), m is a slope-length exponent.

CS refers to the process of vegetation absorbing carbon dioxide through photosynthesis. Therefore, the amount of carbon fixation can be determined according to the process of photosynthesis and the assumption that 1.63 g of carbon dioxide is consumed to produce 1 g of carbon dioxide, expressed as in Eq. (13):

$$CS_i = 1.63 \times A \times NPP \quad (13)$$

where CS_i is the annual fixed amount of CS, t·a^{-1}; A is the area in km^2; *NPP* is Net Primary Production (Table 1), t·km^{-2}·a^{-1}.

2.4. Gradient delineation

The YEB consists of internal variations in the ecological environment and economic development, constituting different gradients. The distribution of ESs across these gradients helps identify spatial differences in ESs. Five gradients were established based on socio-economic and geographic considerations (Table 2): C_E (economic circle), C_D (DEM), C_S (Slope), $C_{U\text{-}D}$ (from upstream to downstream of the Yangtze River), C_R (banks of the Yangtze River).

2.5. Analysis of driving factors

This study mainly used the MGWR method, a regression model for analyzing geospatial data, to study the spatial heterogeneity of the driving factors of ESs in the YEB (Liu et al., 2022b). Different spatial smoothing levels for each variable can more effectively solve the model error caused by changes in different spatial data (Ahmed et al., 2017). This could more effectively explain the spatial interactions between ESs and their driving factors. The model can be expressed as in Eqs. (14)–(15):

$$Y_i = \beta_0(u_i, v_i) + \sum_k \beta_{bwk}(u_i, v_i) X_{ik} + \varepsilon_i \quad (14)$$

$$\varepsilon_i \sim N\left(0, \sigma^2 I\right), i = 1, 2, \cdots, n \quad (15)$$

where y_i is the response variable (ESs) at spatial position (u_i, v_i); X_{ik} is the explanatory variable at spatial position (u_i, v_i); β_0 (u_i, v_i) is the intercept term of the regression relationship. The coefficient β_{bwk} (u_i, v_i) is a continuous function of the spatial position (u_i, v_i). β_{bwk} in *bwk* represents

Table 2
Gradient partitioning method.

Grading code	Classification standard	Classification method	Meaning
C_E	Economic circle	Gradually expanding outwards from the three major economic circles (Chengdu in the Chengdu–Chongqing circle, Wuhan in the middle reaches of the Yangtze River city circle, and Shanghai in the Yangtze River Delta city cluster)	Distance from large urban agglomerations.
C_D	DEM	Elevations and gradients are graded according to natural breakpoints.	Different topographic relief gradients.
C_S	Slope		
$C_{U\text{-}D}$	Upstream to downstream of the Yangtze River	The river basin is graded from top to bottom, and the county of the river basin is assigned a value.	Spatial pattern from west to east.
C_R	Banks of the Yangtze River	Extending north to south along the main body of the Yangtze River, which flows through the central YEB region, extending to both sides of the river north to south.	Distance from the Yangtze River.

Note: C_D and C_S were divided into 11 gradients using 10-point intervals, C_D: 50 m, 150 m, 400 m, 600 m, 900 m, 1200 m, 1500 m, 1800 m, 2400 m, and 3200 m; C_S: 1°, 2°, 3°, 5°, 7°, 9°, 11°, 14°, 17°, and 20°.

the optimal bandwidth of the *k*th independent variable, and ε_i is an independent random error term.

The analysis framework of driving factors was as follows: (1) The Evaluation index system of driving factors is selected by referring to the previous research papers and considering the natural economic conditions of the YEB, establishing and building a database of driving factors with reference to relevant existing studies (Table 3). (2) Use Pearson's correlation to quantify the relationships between different ESs and driving factors and select the higher driving factors. (3) Use MGWR to analyze spatial heterogeneity in the highly correlated driving factors of each ESs.

Table 3
Evaluation index system of driving factors.

Types	Code	Driving factors	Reference
Natural	Tem	Temperature (℃)	(Hu et al., 2022a)
	Pre	Precipitation (mm)	
	ET	Evapotranspiration (mm)	(Huang et al., 2022)
	NDVI	NDVI	(Liu et al., 2022a)
	DEM	Average elevation (m)	
	Slope	Average slope (m)	(Huang et al., 2022)
Geology	Tsand	Proportion of sand (%)	(Liu et al., 2022a)
	Tsilt	Proportion of silt (%)	
	Tclay	Proportion of clay (%)	
	Toc	Proportion of organic matter (%)	
Ecological	PCL	Proportion of cropland (%)	(Li et al., 2022c)
	PWL	Proportion of woodland (%)	
	PGL	Proportion of grassland (%)	
	PWS	Proportion of waters (%)	
	PCS	Proportion of construction land (%)	
Economic	RD	Population density (%)	(Li et al., 2016)
	GPR	GDP per unit area (RMB)	(Wang et al., 2022a)
	FIAV	The output value of the primary industry (RMB)	(Ni et al., 2022)
	SIAV	The output value of the secondary industry (RMB)	
	TIAV	The output value of the tertiary industry (RMB)	
	NL	Night light	(Zhao et al., 2020)

Note: The study unit was identical for each county in the YEB.

2.6. Cluster distribution characteristics of driving factors

The YEB can be divided into regions according to the main driving factors. In order to better describe the differences of natural economic characteristics among different main driving factors. This study quantifies the natural economic characteristics of different regions. A self-organizing map (SOM) was used to perform clustering analysis of driving factors, which encompass various conditions that influence ecosystems, including natural ecology and socio-economic factors. Clustering was implemented using the R package "kohonen" (Wehrens and Kruisselbrink, 2018) (R version 4.1.2). Different ecological and social factors were selected for the different ESs to capture their unique characteristics. Three main environmental factors were chosen, namely the NDVI, Human Influence Index (HAI) (Huang et al., 2019), and Terrain Niche Index (TNI) (Tong et al., 2016). HAI and TNI were calculated using Eqs. (16)–(17):

$$\mathrm{HAI} = \left(\sum_{i=0}^{3} A_i \times P_i \right) \tag{16}$$

where *i* represents the LULC grading index for level *i*, *A* is the area, and P_i represents the LULC proportion. The different land use types and their grading indices were cropland (2), forest (1), water area (1), grassland (1), and construction land (3).

$$\mathrm{TNI} = \log\left[\left(\frac{E}{E_m} + 1 \right) \times \left(\frac{S}{S_m} + 1 \right) \right] \tag{17}$$

where E and S represent the elevation and slope of the grids, respectively; E_m and S_m represent the average elevation and slope of the study area, respectively.

2.7. Threshold effect analysis of driving factors

In the study of ESs, it is believed that the change in ESs reflects the existence of a threshold effect (Rial et al., 2004). In terms of driving factors of ESs, changes in the main driving factors also conform to this theory. To identify the existence of driving factor transformation thresholds, a supervised classification using Linear Discriminant Analysis (LDA) was conducted on the factors (related to MGWR partition), which was implemented using the R package "MASS" (Venables and Ripley, 2002).

3. Results

3.1. Spatial patterns of ecosystem services

Using counties as statistical units, the average functional values of ESs per unit area from 2000 to 2020 were as follows: 403 mm for WY; 9897 t·km^{-2} for SC; 1071 g·CO_2·m^{-2} for CS, respectively. Pronounced spatial heterogeneity was observed among three ESs (Fig. 2, Fig. A1). WY (Fig. 2a) was significantly lower in the north and west areas of the Yangtze River than the south and east. The spatial distribution of SC (Fig. 2b) showed that high values were mainly distributed on plateaus or in hilly areas, with the largest SC values found in the western region. In certain low mountainous and hilly regions of the southern area, there are also areas where SC was relatively high. Overall, the spatial distribution of SC showed a pattern similar to that of the region's topography I and that of CS. The highest values of SC were concentrated in the high-elevation areas (around the Yungui Plateau), while low-value areas were mainly flat regions (e.g., the Sichuan Basin, and Poyang Lake Plain). The high-elevation areas (e.g., western Sichuan Plateau) corresponded to

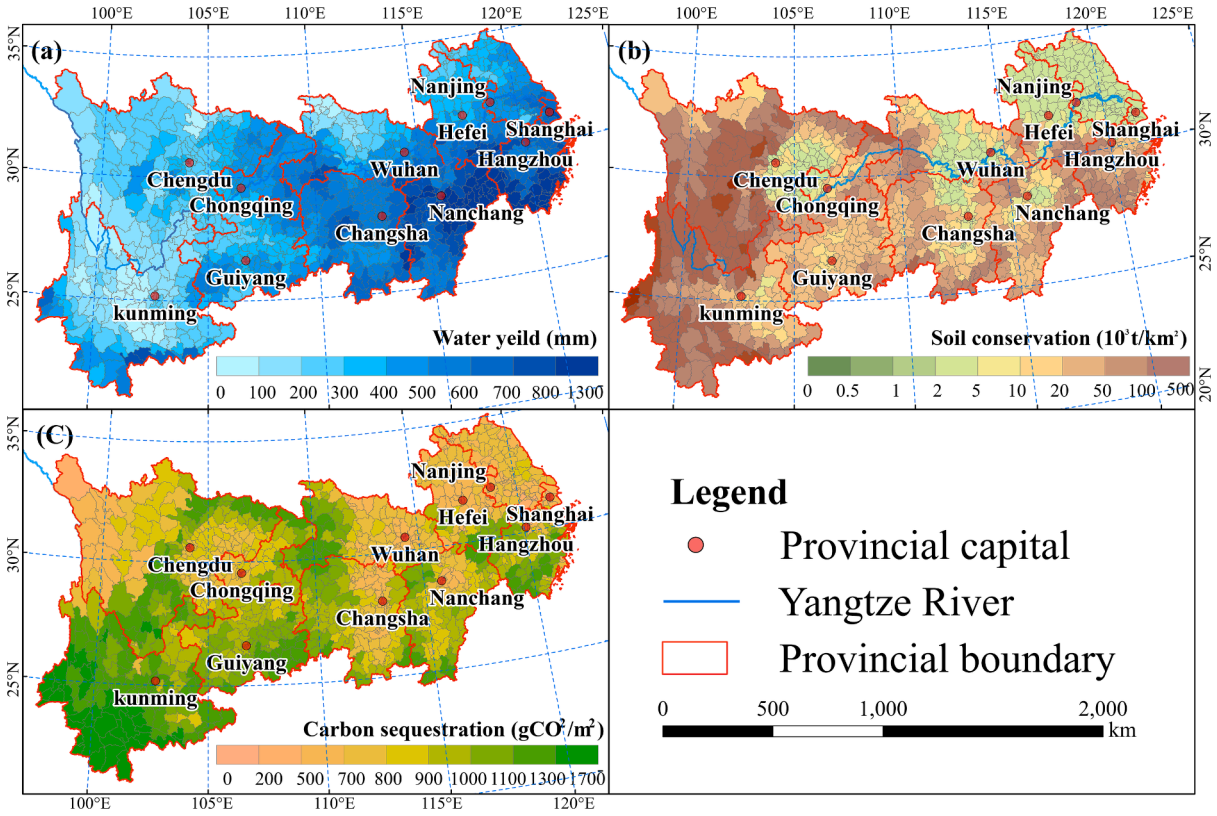

Fig. 2. Annual average ESs from 2000 to 2020. (a) spatial distribution of the annual mean value of water yield; (b) spatial distribution of the annual mean value of soil conservation; and (c) spatial distribution of the annual mean value of carbon sequestration.

areas of low SC values (Fig. 2c).

3.2. Gradient distribution of ecosystem services

WY increased with the gradients of C_E, C_D, and C_S, but decreased with the gradients of $C_{U\text{-}D}$ and C_R. SC showed a downward trend in the C_E, C_D, and C_S gradients, an upward trend in the $C_{U\text{-}D}$ gradient, and a single-peak curve change in the C_R (Fig. 3e.2). CS showed an upward trend under the C_E gradient and a downward trend under the $C_{U\text{-}D}$ gradient. The C_D and C_S gradients showed a single-peak curve that first increased and then decreased, while the C_R gradient showed a single-peak curve that first decreased and then increased (Fig. 3e.3). Compared with SC and CS, the change trend of WY on each gradient was almost opposite, and the response to the C_R gradient change was more pronounced. For SC and CS, the change in the terrain gradient and the difference between the low and high terrain gradients were evident. The rate of increase in SC becomes greater with an increase in C_D, and C_S. SC and CS had their minimum values in the region near the Yangtze River, which were approximately in the N1–S1 range (Fig. 3e.2 and Fig. 3e.3).

3.3. Driving factors of ecosystem services

WY was negatively correlated with SC (-0.12) and CS (-0.29), and SC was positively correlated with CS (+0.40). WY was positively correlated with meteorological factors (Pre) and economic indicators (NL) and negatively correlated with topographic factors (DEM, Slope). The indicators related to SC and natural ecology were mainly positively correlated (NDVI, DEM, Slope, PWL, and PGL), whereas those related to human activities were mainly negatively correlated (PCL). Similar patterns were found for CS and SC. In general, natural factors (NDVI, DEM, Slope), whereas the social-economic indicators (PCL, PWS, and NL) were negatively correlated with services. The top six driving factors for ESs based on the magnitudes of their correlation values are presented in Supplementary Data (Table A2).

ANOVA reveals the contribution of the highly correlated driving factors on ESs (Table 4). Main contributing indicators were as follows: Pre (55.30 %), Tem (18.36 %), DEM (14.32 %); SC: DEM (52.60 %), Slope (21.50 %), NDVI (18.60 %) for WY; DEM (52.60 %), Slope (21.50 %), NDVI (18.60 %) for SC; NDVI (83.10 %), DEM (10.80 %), Slope (4.80 %) for CS. The results indicate that factors exhibiting high correlation typically exhibited higher contribution rates. However, within indicators showing similar levels of correlation, certain factors emerged as dominant contributors. For instance, NDVI contributes more than 80 % to the CS, significantly surpassing other highly correlated factors such as DEM and Slope.

3.4. Spatial distribution of driving factors

Using the AIC, AICC, and R^2 to test the OLS and MGWR models, the results showed that the MGWR model more effectively described the driving patterns of ESs factors in the YEB (Table 5). The specific process and description of MGWR are placed in Additional File 1 and Fig. A4 of the Supplementary Data.

The main driving factors of WY could be divided into seven categories (Fig. 4a): M1 (DEM and Tem), M2 (DEM and Slope), M3 (DEM and Pre), M4 (DEM and NL), M5 (Pre and Tem), M6 (Pre and DEM), and M7 (Pre and NL). According to WY, the YEB could be divided into two parts based on the first main driving factor. The first region, located in the eastern and central areas, was primarily driven by DEM (M1, M2, M3, and M4). The second region, located in the western area, had Pre as the main driving factor (M5, M6, and M7). However, based on spatial patterns, they could be divided into three regions. The first consisted of M1 and M2, which were concentrated in the eastern region; the second consisted of M5 and M7, which were concentrated in the western part. M3, M4, and M6 were transitional areas between these two main regions, with fragmented spatial patterns.

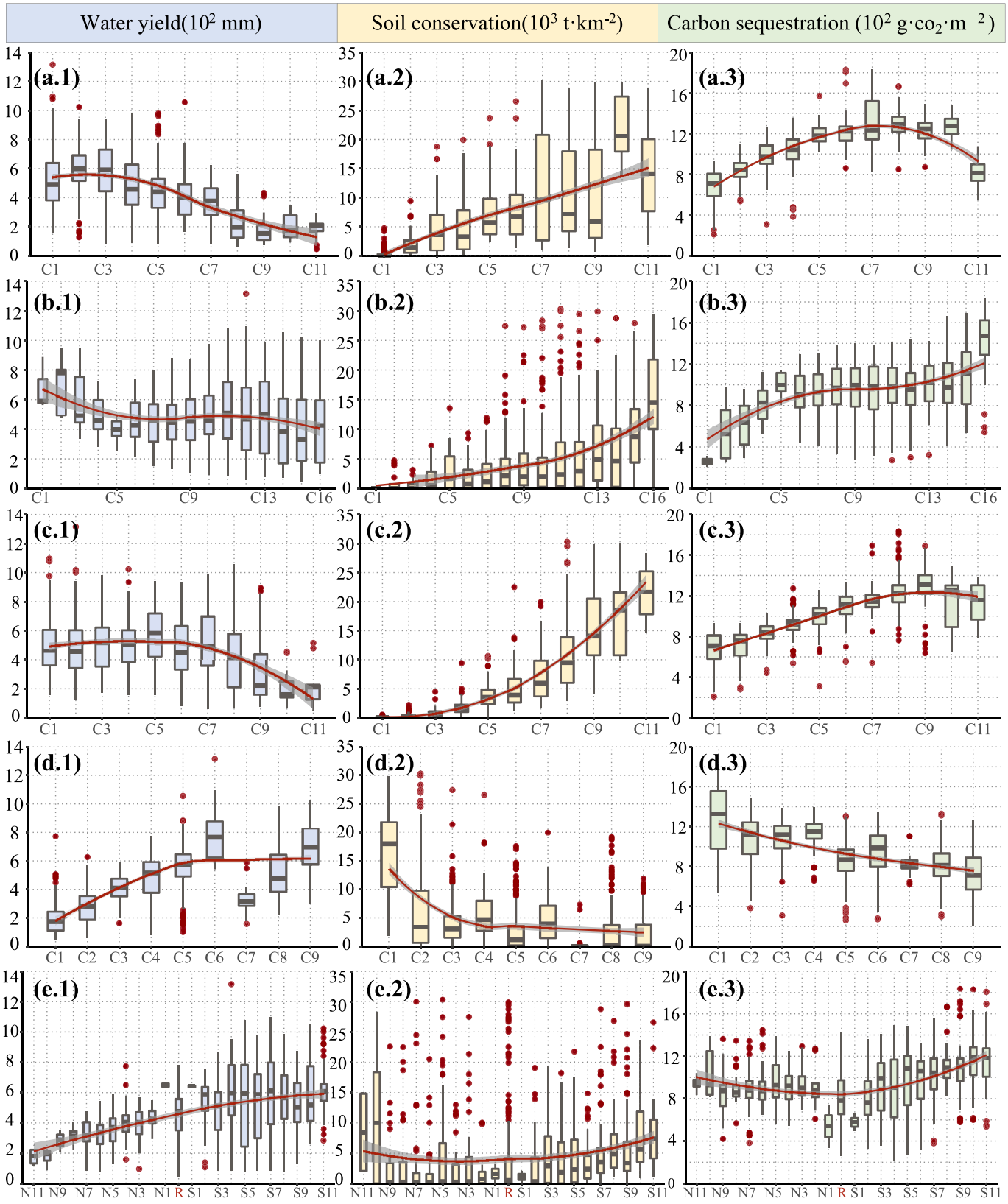

Fig. 3. Distribution of ecosystems on different gradients. The gradient types are respectively: (a) circle of economics; (b) circle of DEM; (c) circle of Slope; (d) circle of upstream to downstream of the Yangtze River; (e) circle of banks of the Yangtze River. The red circles represent outliers, the red lines represent the fitted curve, shadow regions represent 95 % confidence intervals. (For interpretation of the references to colour in this figure legend, the reader is referred to the web version of this article.)

Table 4
Contribution of highly correlated driving factors.

WY	Driving Factor	Pre	Tem	DEM	NL	Slope	PGL
	Contribution	55.30 %	18.36 %	14.32 %	7.62 %	4.34 %	0.06 %
SC	Driving factor	DEM	Slope	NDVI	PGL	PWL	PCL
	Contribution	52.60 %	21.50 %	18.60 %	6.00 %	0.90 %	0.30 %
CS	Driving Factor	NDVI	DEM	Slope	PCL	PWS	NL
	Contribution	83.10 %	10.80 %	4.80 %	1.10 %	0.00 %	0.20 %

The main driving factors of SC could be divided into four categories (Fig. 4b): M1 (NDVI and Slope), M2 (NDVI and PWL), M3 (Slope and PWL), and M4 (Slope and PGL). The primary drivers were represented by M3 and M4, with M3 occupying most of the YEB and M4 mainly distributed in parts of the Jiangxi, Hunan, and Sichuan provinces and Chongqing Municipality. Regions M1 and M2 were concentrated in the southern part of Yunnan Province and the central part of Sichuan Province.

The main driving factors of CS could be divided into four categories (Fig. 4c): M1 (NDVI and DEM), M2 (NDVI and Slope), M3 (NDVI and PWL), and M4 (NDVI and NL). The primary factor in each region was the NDVI, and based on secondary driving factors, they could be divided into two types. M1 and M2 were mainly related to terrain factors and primarily distributed in the western part of the YEB. Further, there was a focus on the southern part of Hunan Province, Guizhou Province, Chongqing Municipality, the northern part of Sichuan Province, and Yunnan Province. M3 and M4 were mainly influenced by land cover and socio-economic factors and primarily distributed in the eastern part of the YEB and the southern part of Sichuan Province.

3.5. Cluster analysis of driving factors

To determine the association between the spatial heterogeneity of driving factors of ESs and their clustering characteristics, a cluster analysis each ESs driving factor was carried out. TNI, NDVI, HAI, and other indicators were selected to represent the terrain, ecology, and human activities in the region. Specific driving factors were selected for each ESs (Table A2), with Pre selected for WY, PWL for SC, and NL for CS.

The clustering results for WY exhibited different characteristics (Fig. A5). B1 indicated a high NDVI, TNI and low human impacts; B2 showed high NDVI; B3 showed high human impacts; and B4 showed high precipitation and high NDVI. The clustering results could be divided into three regions, similar to the MGWR classification results (Fig. 4). The clustering results of M1 and M2 differed significantly from those of M5, M6, and M7, whereas the clustering results of M3 and M4 were intermediate. In M1 and M2, B4 and B2 were more prevalent. M3 and M4 represented transitional zones between the other two regions and had a fragmented distribution pattern. M5, M6, and M7 were located in the western region, where the clustering results were dominated by B1 and B2. The prevalence of B1 clustering gradually decreased in M5, M7, and M6, whereas that of B2 gradually increased.

The characteristics of the four clustering results of SC were as follows. B1 indicated high forest coverage and high NDVI; B2 showed high NDVI; B3 showed high anthropogenic influence; and B4 showed high TNI and NDVI. The statistical results clearly fell into two main categories and were consistent with the MGWR classification results (Fig. 4). M1 and M2 were primarily composed of B4, whereas M3 and M4 were composed of B1 and B2.

The spatial distribution of CS, divided by its secondary driving factor, exhibited a clear east to west pattern. M1 and M3, the two categories with the largest percentage area in the MGWR classification results (Fig. 4), also differed greatly in their clustering results (Fig. A5). In M1, the main clustering type was B4; however, some regions were also classified as B1. Compared with the other categories, M3 had a higher proportion of B1 and moderate proportions of B2 and B3. Topographic factors in this region were not prominent, indicating a greater influence of anthropogenic factors.

4. Discussion

4.1. Result of ESs

The accounting results of ecosystem services are affected by many factors. The results of other researchers are selected for comparison to determine the availability and reliability of the ESs accounting results. The WY results obtained in this study were consistent with the actual runoff in the Yangtze River Basin, with a difference of 20 % (8.2×10^{11} m^3 compared with 9.85×10^{11} m^3, respectively) (China National Bureau of Statistics, 2021). The disparities in the results can be attributed to differences in the spatial extent and inconsistencies in the statistical timeframe. The calculated SC results in this study were in basic agreement with the findings of previous research conducted in the same region (Wu et al., 2018), with a 6 % difference (2.02×10^{10} t compared with 1.88×10^{10} t, respectively). The calculated CS results were consistent with the findings of a previous study conducted in the same region (WU et al., 2021), with a 15 % difference (1071 $g{\cdot}CO_2{\cdot}m^{-2}$ compared with 903.35 $g{\cdot}CO_2{\cdot}m^{-2}$, respectively). We speculate that discrepancies in data sources and study period (2010–2015) contributed to the observed differences in the original data.

4.2. Driving mechanisms of ecosystem services

WY exhibited a pattern of higher values in the southeast and lower values in the northwest (Hu et al., 2022c). Regions with higher WY

Table 5
Parameters for the MGWR model.

WY			SC			CS		
Verification indicators	OLS	MGWR	Verification indicators	OLS	MGWR	Verification indicators	OLS	MGWR
AIC	815.01	3.18	AIC	2658.02	2256.88	AIC	1292.78	−1284.03
AICC	817.15	112.72	AICC	2660.19	2281.48	AICC	1294.95	−1214.72
R^2	0.88	0.95	R^2	0.31	0.61	R^2	0.81	0.99
DF	Bandwidth	t (95 %)	DF	Bandwidth	t (95 %)	DF	Bandwidth	t (95 %)
Intercept	43	3.09	Intercept	1069	2.00	Intercept	43	3.22
Tem	43	3.16	NDVI	57	3.23	NDVI	43	3.28
DEM	43	3.07	DEM	1069	2.01	DEM	43	3.22
Slope	43	3.19	Slope	969	2.07	Slope	1063	1.99
Pre	43	3.15	PCL	1069	1.99	PWL	43	3.27
PGL	43	3.21	PWL	43	3.36	PWS	377	2.41
NL	43	3.21	PGL	1069	2.04	NL	605	2.15

Note: The top half of the table is the comparison of MGWR and OLS models, and the bottom half is the bandwidth and t-tests for different drivers.

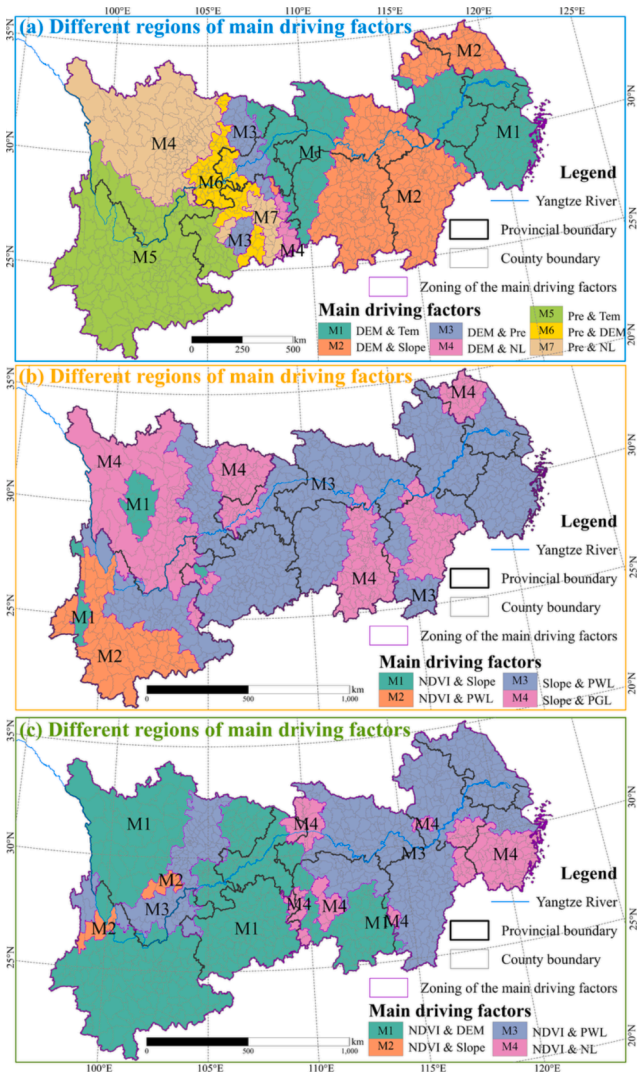

Fig. 4. Spatial distribution of the main driving factors. Figures shows the spatial distribution of the main driving factors for each region, figure a is water yield, figure b is soil conservation, figure c is carbon sequestration. M1-M7 represents regions of the same primary driver (The partition process in Supplementary Data Fig. A4).

tended to coincide with areas of high human activity, such as provincial capitals, as indicated in Fig. 3. Local studies within the YEB, such as those in the Xiangjiang (Wang et al., 2023c) and Weihe river basins (Wu et al., 2022a), have also confirmed a decreasing trend in WY, as shown in the C_E (Fig. 3). The main factors influencing WY were Pre (55.30 %), Tem (18.36 %), DEM (14.32 %), and NL (7.52 %). These findings were consistent with those of other studies (Wang et al., 2021) indicating Pre as the dominant factor influencing the spatial distribution of WY (Wang et al., 2023). Specifically, Pre affects the regional water input and surface hydrological processes, leading to changes in runoff and influencing the WY spatial distribution (Wang et al., 2022c). The impact of Tem and WY in the YEB was positively correlated, which was consistent with research at the national level (Gong et al., 2017). However, Tem can increase evapotranspiration and decrease runoff (Su and Fu, 2013; Wei et al., 2022). Thus, the combined effects of Tem and factors such as Pre and DEM can result in the opposite effect of Tem in the YEB. Existing research has indicated a positive correlation between Tem and WY in regions with ample precipitation, such as Guizhou with 1630 mm in 2020 (Wang et al., 2023), while a negative correlation is observed in drier areas like the Shule River Basin, which received 47–63 mm of precipitation (Wei et al., 2022). Our study generally aligns with these findings, as the YEB has abundant precipitation (1392 mm, 2020) and demonstrates a positive relationship (Fig. A3). Terrain factors incorporate the influence of human activities (NL) on the spatial distribution of WY at a smaller scale (Sun et al., 2021). They can affect precipitation, temperature, and other conditions, resulting in human activity being concentrated in low altitude and slope areas. Factors such as accelerated urbanization have also altered the underlying surface, increased surface impermeability and enhanced WY (Khzr et al., 2022). In addition, the terrain affects runoff flow, causing it to accumulate in flat areas.

The spatial distribution pattern of SC was generally a low in the east and high in the west, showing a gradual increase with an increase in C_D (Fig. 3b.1) and C_S (Fig. 3c.1). Variations along these two gradients were more regular and exhibited higher levels of dispersion. The contributions of high correlation driving factors to SC (Table 4) indicated that topographic factors accounted for approximately 74.1 % of the variance and served as the dominant driving factors of the spatial distribution of SC (Xiao et al., 2017). This conclusion is consistent with existing research on the Yangtze and Yellow River basins (Fang et al., 2021). Slope is an important factor that affects runoff, with higher slopes having a greater potential for soil erosion (Yan et al., 2018). Moreover, regions with higher slopes tend to have less human activity and greater vegetation cover. DEM is one of the main factors influencing the spatial distribution of SC (Chen et al., 2023), and variations in multiple conditions, such as human activities and weather, along the vertical gradient lead to differences in vegetation cover at different altitudes (Chen et al., 2023; Liu et al., 2007), resulting in greater vegetation growth at higher altitudes and higher soil retention capacity. The NDVI is also seen as a direct influencing factor (Liu et al., 2022c) because higher vegetation cover could mitigate soil erosion through factors such as a reduced impact of raindrops, lower surface runoff velocity, stable soil particles, and increased soil water holding capacity. Therefore, it had a positive correlation with SC.

CS exhibited a spatial pattern with higher values in the south and west and lower values in the north and east, except for the Sichuan Basin, where CS was relatively low. The main driving factors with a high correlation with CS were the NDVI, DEM, Slope, and PCL, among which the NDVI was the most significant factor (Table 4), explaining 83.1 % of the variance; topographic factors accounted for 15.6 %. Thus, the NDVI, influenced by factors such as meteorological conditions, topography, and human activity (Li, 2022), played a dominant role in the spatial distribution of CS. Precipitation had a positive effect on the NDVI, because higher precipitation meets plant growth needs. In turn, temperature had a negative impact on the NDVI because regions with higher temperatures are more suitable for human habitation, and excessive human activity can lead to a decrease in the NDVI (Han and Xu, 2013). The gradient boxplot of the DEM (Figs. 3-b.4) indicated a two-stage distribution pattern for CS. In the first stage, as human impacts gradually decreased, CS increased. With the increase of DEM, unfavorable natural conditions, such as decrease in temperature and precipitation, impede vegetation growth (Chen et al., 2020), resulting in a decrease in CS (Zhang et al., 2020). Therefore, the Sichuan Basin (200–700 m) with a lower DEM and the western Sichuan Plateau (4000–4500 m) exhibited lower CS. Compared with other ESs, CS was more significantly affected by human activities, with larger differences in various gradients of land-use changes (C_E) (Fig. 3a.3) and higher Pearson correlation coefficients.

4.3. Spatial differences in ecosystem service driving factors

The main driving factors of WY showed significant spatial variation, with China's topographic boundary (second and first gradients) as the dividing line. In the eastern region, the DEM was the main driving factor, whereas in the western region, Pre was the main driving factor, with a transitional zone near the boundary. The contribution of the two factors was 73.66 % (Table 4). The results of the majority of scholars also concluded that precipitation is considered to be the most important factor affecting WY (Fig. 4). However, topography could affect the

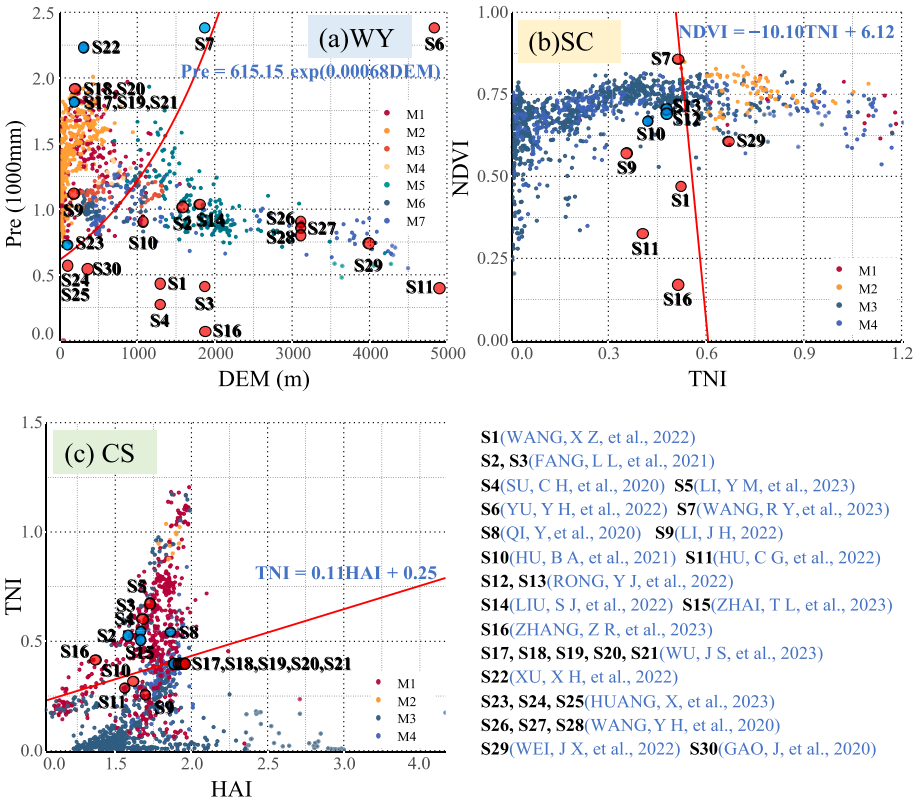

Fig. 5. Linear Discriminant Analysis of driving factors. Based on the previous partitioning method, the zoning results of the MGWR for each ecosystem service were divided into two regions, C1 and C2. For WY, C1 (M1 & M2 & M3 & M4), C2 (M5 & M6 & M7); for SC, C1 (M1 & M2) and C1 (M3 & M4); and for CS, C1 (M1 and M2) and C1 (M3 & M4). The threshold of the transformation of the drivers is shown in the formula. The conformity rates with the zoning results of MGWR are: WY (84.76 %), SC (86.53 %), SC (80.04 %). The results of the other papers are plotted on a graph, where red points indicate agreement with the findings of this paper and blue points indicate disagreement. (For interpretation of the references to colour in this figure legend, the reader is referred to the web version of this article.)

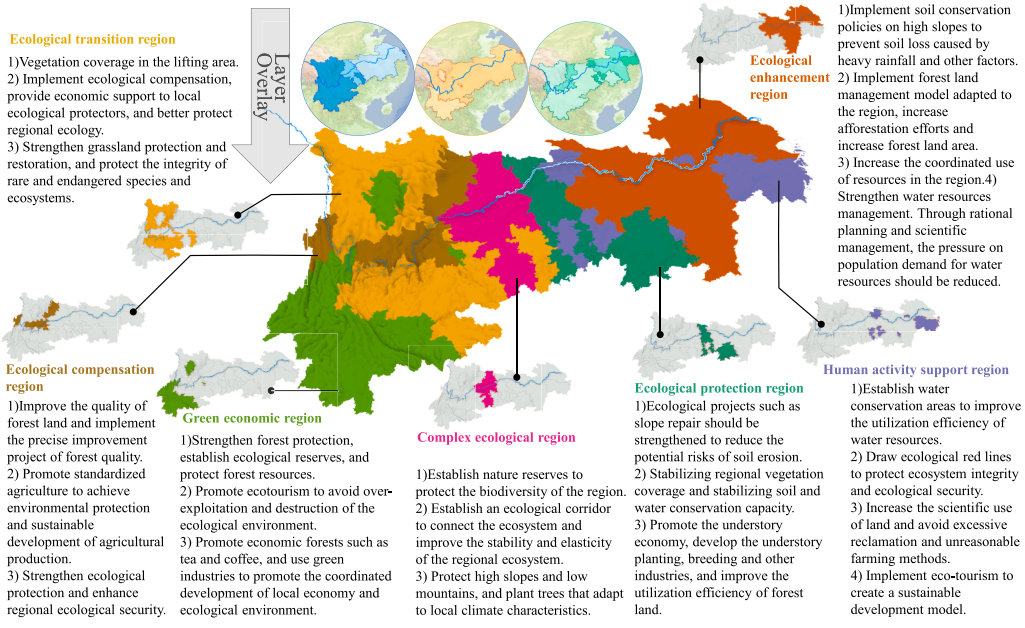

Fig. 6. Zoning management of ecosystem conservation.

importance of precipitation in driving WY (Dai and Wang, 2020). In our study, the clustering results of WY (Fig. A5) indicated that regions with suitable ecological conditions (B2) and higher precipitation (B4) were mainly driven by DEM, whereas regions with lower human impacts, higher vegetation cover (B1, B2), and insufficient precipitation (B1, B2) were mainly driven by Pre. The main reason for this phenomenon was that precipitation and topography were negatively correlated. Most areas of the YEB, which had a high DEM, were strongly influenced by the

plateau mountain climate, with less precipitation and more evaporation. Therefore, Pre became the determining factor of WY. In contrast, in the eastern region, which is influenced by the monsoon climate, precipitation is abundant, and DEM performed a greater impact on the distribution of WY in the region. The results of the linear discriminant analysis (Fig. 5a) indicated that the higher the precipitation, the greater the likelihood that the DEM is the main driving factor, whereas areas with higher DEM were mainly driven by Pre. This conclusion is consistent with the results of the MGWR model (Fig. 4), and the consistency between the two zoning methods was approximately 86.53 % (Fig. 5a). To ensure the robustness of these findings, we conducted a comprehensive review of all available reference related to the driving factors of WY. We meticulously compiled and recalculated their results (Fig. 5a, detailed data available in Table A3). Researchers' findings not only depict the temporal variations of WY's primary driving factors but also align with our proposed transition threshold curve in 70 % of cases. For instance, Wu et al. (2023) revealed that in the Pearl River region, with changing precipitation values, the primary driving factor for WY transitions from DEM to Pre.

The NDVI, Slope, and DEM are the main factors affecting SC (Wang et al., 2022b), and the primary driving factor of these remains controversial. The combined contribution of the factors is 92.70 % (Table 4). Some researchers have suggested that slope is the main driving factor (Hu et al., 2022b; Li, 2022), while other studies have attributed this to the NDVI (Mu et al., 2022). In this study, SC clustering results were statistically significant (Fig. A5). In areas where the NDVI was the main driving factor, there were more clusters with a high terrain gradient, and the corresponding NDVI was the main factor in the cluster. The primary driving factor was the terrain factor, that is, the slope. This pattern is consistent with research on the Pearl River Delta region (Liu et al., 2022c), mainly because the slope can affect the CS capacity of the region by affecting runoff and surface vegetation. Most regions where the NDVI is the main driving factor are plateaus, such as the Yunnan-Guizhou Plateau, where vegetation cover is low and the impact of vegetation changes is greater. The results of the linear discriminant analysis (Fig. 5b) indicated that the larger the TNI value in an area, the greater the likelihood that the NDVI is the main driving factor; the higher the NDVI in an area, the more likely it is that the slope is the main driving factor. This conclusion is consistent with the results of the MGWR model (Fig. 4a), with the consistency between the two zoning methods being approximately 84.76 % (Fig. 5b). We have also made exhaustive efforts to systematically review literatures on SC driving factors in Fig. 5b (also see Table A2). Researchers' findings similarly demonstrate changes in the primary driving factors for SC, with 66.7 % of results aligning with our proposed transition threshold curve. We conducted a thorough analysis of studies that exhibited discrepancies, e.g., Rong et al. (2022), and found that these discrepancies were typically associated with larger-scale investigations. Larger-scale studies often average the values of TNI due to computational precision issues, which constitutes a primary reason for discrepancies with the results presented in this study.

The MGWR results for CS (Fig. 4c) indicated that the main driving factor of CS is the NDVI (Ge et al., 2021; Ye et al., 2022). Using the second main driving factors as the classification basis, the YEB was divided into two regions: the western region mainly driven by topography (DEM and Slope) and the eastern region mainly driven by human activities (PWL and NL). However, there has been a lack of discussion regarding the main driving factors of CS. The impact of human activity in the Pearl River Delta region is greater than that of topography (Liu et al., 2022c), whereas research in northeastern China yielded the opposite results (Sun et al., 2018). The clustering results of CS (Fig. 5c) indicated that clustering in the western region was mainly characterized by a high TNI and NDVI, whereas in the eastern region, human activities (B2) and a high NDVI (B1) had a relatively larger effect. This was consistent with the regional characteristics of the Pearl River Delta in northeastern China. Further, linear discriminant analysis (Fig. 5c) showed that the higher the TNI value in an area, the greater the likelihood that the NDVI is the main driving factor, whereas the higher the HAI value in an area, the more likely it is that human activities are the main driving factor. This conclusion is consistent with the results of the MGWR model, with the consistency between the two zoning methods being approximately 80.04 % (Fig. 5a). Previous research studies have corroborated the primary driving factor transition pattern presented in this paper, with a concurrence rate of 66.7 % (Fig. 5c, Table A3). For instance, Wu et al. (2023), who conducted a similar study in Pearl River Delta of China, observed that with the increasing intensity of human activities (HAI), anthropogenic factors gradually supplant topography (TNI) as the predominant drivers influencing SC.

4.4. Ecosystem service management advice

ESs can serve as vehicles for shaping the value of natural resources through spatial planning and provide a cognitive foundation for value shaping in spatial planning (Carpenter et al., 2009). The spatial heterogeneity of the impacts on ESs reflects comprehensive differences in regional conditions, such as ecological and socio-economic factors. Therefore, to achieve sustainability of the ecosystem's provisioning capacity in the YEB, optimize the regional industrial layout, and promote coordinated development among regions, the spatial layout of driving factors should be the primary basis for spatial planning, considering the differences in ESs. This will help propose spatial planning and corresponding management measures for the YEB. To divide the counties in the YEB, a zoning method should be used. Regions with similar main driving factors of ESs should be merged, and the three ESs can be divided into different zones. After overlaying the three zones, ecosystem conservation management zones for the YEB can be generated (Fig. 6) and management strategies based on the characteristics of each zone can be proposed. The specific partitioning strategy is shown below: First, the YEB is divided into multiple regions based on the primary driving factors of ecosystem services. Specifically, WY is divided into three regions: 1 (M1 & M2), 2 (M3 & M4 & M6), and 3 (M5 & M7), with Region 2 serving as a transitional zone; SC is divided into two regions: 1 (M1 & M2) and 2 (M3 & M4); CS is divided into three regions: 1 (M1), 2 (M2 & M3), and 3 (M4). Finally, we overlay the respective regions and label the overlaid areas in the order of WY, SC, and CS, using the following numbers for each region: 121 (Ecological protection region), 122 (Ecological Enhancement region), 123 (Human activity support region), 221 (Complex ecological region), 311 (Green economic region), 321 (Ecological transition region), and 322 (Ecological compensation region).

The characteristics and policy priorities of each region are as follows. **Ecological transition region** is an area of excessive transition from the Yangtze River Economic Belt to the northern plateau region. The ecosystem in this area is gradually becoming fragile, so emphasis is placed on protecting vegetation coverage, which were also acknowledged by literature (Yang et al., 2021). **Ecological compensation region**, PWL affects the SC and CS of the region, so the region is dominated by forest construction and ecological conservation. **Green economic region** is ecologically sound and has the basis for the transformation of good ecology into regional economic development and the implementation of conservation and development policies. Studies in this region (Yunnan Province) indicate that the development of ecotourism in this area promotes the integrated development of ecology and economy (Zhu et al., 2023). **Complex ecological region** is influenced by multiple factors, and the ecological situation is complex. Policies focus on protecting the region's biodiversity. **Ecological protection region**: Due to terrain factors, soil erosion is severe in this region, and a significant amount of ESs is needed. Therefore, emphasis is placed on regional security construction. Research in this region (Jiangxi Province) shows that soil and water conservation measures aid in mitigating water and soil erosion in the region (Tu et al., 2018). **Human activity support region**, human activities are important influencing factors in this region, and the supply capacity of WY is also high. Therefore,

attention is paid to water source and environmental protection, as well as planned and efficient land use. **Ecological enhancement region**: this region is an important grain production area, and the primary influencing factor of ESs is PWL. Therefore, the balance between agricultural development and forest construction is emphasized, as well as the protection of ecological redlines and cultivated land redlines.

4.5. Limitation and prospect

There are limitations and uncertainties in the models and results of ESs calculations, and although this study chose the InVEST model, which is the most widely used model in the world (Kareiva et al., 2011), and searched for a number of studies to localize the parameters, the impacts of regional variability on large scales should not be ignored (Ren et al., 2022). This study focuses more on spatial scale variability and less on temporal scale changes, on the one hand, because the 20-year study timeframe is still relatively short, and the magnitude of land use changes in the overall region is small, and the regularity of climate change is not yet strong, on the other hand, for the Yangtze River Economic Belt as a special region, the spatial variability of ecosystem services caused by the variability of the natural and social elements is more significant. In the future, longer time span data and regionally different parameters can be used to study climate change or land use change within the same region.

5. Conclusion

ESs have been considered in large-scale policy decision making, but there is a high level of spatial heterogeneity in ESs and their driving factors. This affects the applicability of policies to various regions to a certain extent. This study used geospatial and panel data and classical models to quantify WY, SC, and SC as well as the primary driving factors. As one of the rare studies that considered drivers transformation patterns, we found that the YBE showed spatial heterogeneity of ESs and drivers, and this can be quantified. The YEB showed spatial heterogeneity in ESs and driving factors and there was consistency in its layout from the perspective of spatial distribution patterns. Therefore, a spatial division of ESs management was proposed based on the spatial division of driving factors, and the characteristic management strategies of each region were constructed. This is likely to have a forward-looking effect on the quantitative implementation of ecosystem zoning management, policy economy, and environmental protection policies in the region and provide a reference for the sustainable use of regional and global ecosystems. Additionally, it is worthwhile to highlight the methodological novelty used in this present study. The first, we showed the high interest of using self-organizing maps (SOM) in depicting both ESs and their drivers at large geographical scale. Second, we showed the appropriateness of the Linear Discriminant Analysis method in determining thresholds of driving factor transitions and generating threshold curves (Fig. 5). Using these methods in conjunction will be greatly helpful for a better understanding of large-scale ESs patterns and underlying mechanisms in future studies.

CRediT authorship contribution statement

Zeyang Xie: Conceptualization, Formal analysis, Methodology, Validation, Visualization, Writing – original draft. **Liujie He:** Data curation, Validation. **Zhun Mao:** Conceptualization, Supervision, Writing – review & editing. **Wei Wan:** Funding acquisition, Project administration, Visualization. **Xu Song:** Methodology. **Zhijian Wu:** Methodology. **Han Liang:** Methodology. **Jing Liu:** Data curation. **Bofu Zheng:** Funding acquisition, Investigation, Methodology. **Jinqi Zhu:** Conceptualization, Supervision, Writing – review & editing.

Declaration of competing interest

The authors declare that they have no known competing financial interests or personal relationships that could have appeared to influence the work reported in this paper.

Data availability

Data will be made available on request.

Acknowledgement

This work was supported by the National Natural Science Foundation of China (32201626, 42301091), the Key Research and Development Program of Jiangxi Province (20223BBG74S01, 20223BBG71013).

Appendix A. Supplementary data

Supplementary data to this article can be found online at https://doi.org/10.1016/j.ecolind.2024.111729.

References

Abdul-Rahim, A.S., Sun, C.L., Noraida, A.W., 2018. The impact of soil and water conservation on agricultural economic growth and rural poverty reduction in china. Sustainability 10 (12). https://doi.org/10.3390/su10124444.

Ahmed, M., Abd-Elrahman, A., Escobedo, F.J., Cropper, W.P., Martin, T.A., Timilsina, N., 2017. Spatially-explicit modeling of multi-scale drivers of aboveground forest biomass and water yield in watersheds of the southeastern united states. J. Environ. Manage. 199, 158–171. https://doi.org/10.1016/j.jenvman.2017.05.013.

Bai, Y., Jiang, B., Wang, M., Li, H., Alatalo, J.M., Huang, S.F., 2016. New ecological redline policy (erp) to secure ecosystem services in china. Land Use Policy 55, 348–351. https://doi.org/10.1016/j.landusepol.2015.09.002.

Bao, H.J., Wang, C.C., Han, L., Wu, S.H., Lou, L.M., Xu, B.G., Liu, Y.F., 2020. Resources and environmental pressure, carrying capacity, and governance: a case study of yangtze river economic belt. Sustainability 12 (4). https://doi.org/10.3390/su12041576.

Bardgett, R.D., Bullock, J.M., Lavorel, S., Manning, P., Schaffner, U., Ostle, N., Chomel, M., Durigan, G., Fry, E.L., Johnson, D., Lavallee, J.M., Le Provost, G., Luo, S., Png, K., Sankaran, M., Hou, X.Y., Zhou, H.K., Ma, L., Ren, W.B., Li, X.L., Ding, Y., Li, Y.H., Shi, H.X., 2021. Combatting global grassland degradation. Nat. Rev. Earth Environ. 2 (10), 720–735. https://doi.org/10.1038/s43017-021-00207-2.

Berdugo, M., Delgado-Baquerizo, M., Soliveres, S., Hernandez-Clemente, R., Zhao, Y.C., Gaitan, J.J., Gross, N., Saiz, H., Maire, V., Lehman, A., Rillig, M.C., Sole, R.V., Maestre, F.T., 2020. Global ecosystem thresholds driven by aridity. Science 367 (6479), 787. https://doi.org/10.1126/science.aay5958.

Carpenter, S.R., Mooney, H.A., Agard, J., Capistrano, D., Defries, R.S., Diaz, S., Dietz, T., Duraiappah, A.K., Oteng-Yeboah, A., Pereira, H.M., Perrings, C., Reid, W.V., Sarukhan, J., Scholes, R.J., Whyte, A., 2009. Science for managing ecosystem services: beyond the millennium ecosystem assessment. Proc. Natl. Acad. Sci. u. s. a. 106 (5), 1305–1312. https://doi.org/10.1073/pnas.0808772106.

Chen, W., Bian, J., Zhong, M., Zeng, J., Liang, J., Zeng, Y., 2022. Impact of traffic accessibility on ecosystem health: a case study of the middle reaches of the yangtze river urban agglomerations. Acta Ecologica Sinica 42 (14), 5721–5733.

Chen, S.S., Ma, M.H., Wu, S.J., Tang, Q.Q., Wen, Z.F., 2023. Topography intensifies variations in the effect of human activities on forest npp across altitude and slope gradients. Environ. Dev. 45 https://doi.org/10.1016/j.envdev.2023.100826.

Chen, T., Xia, J., Zou, L., Hong, S., 2020. Quantifying the influences of natural factors and human activities on ndvi changes in the hanjiang river basin, china. Remote Sens. 12 (22) https://doi.org/10.3390/rs12223780.

China National Bureau of Statistics, 2021. 《statistical yearbook of yangtze river economic zone 2020》. China Statistics Press. https://doi.org/10.38715/y.cnki.ycjjd.2022.000001.

Comberti, C., Thornton, T.F., Echeverria, V.W., Patterson, T., 2015. Ecosystem services or services to ecosystems? Valuing cultivation and reciprocal relationships between humans and ecosystems. Glob. Environ. Change-Human Policy Dimens. 34, 247–262. https://doi.org/10.1016/j.gloenvcha.2015.07.007.

Costanza, R., Darge, R., Degroot, R., Farber, S., Grasso, M., Hannon, B., Limburg, K., Naeem, S., Oneill, R.V., Paruelo, J., Raskin, R.G., Sutton, P., Vandenbelt, M., 1997. The value of the world's ecosystem services and natural capital. Nature 387 (6630), 253–260. https://doi.org/10.1038/387253a0.

Dai, E.F., Wang, Y.H., 2020. Attribution analysis for water yield service based on the geographical detector method: a case study of the hengduan mountain region. J. Geogr. Sci. 30 (6), 1005–1020. https://doi.org/10.1007/s11442-020-1767-y.

Donohue, R.J., Roderick, M.L., Mcvicar, T.R., 2012. Roots, storms and soil pores: incorporating key ecohydrological processes into budyko's hydrological model. J. Hydrol. 436–437, 35–50. https://doi.org/10.1016/j.jhydrol.2012.02.033.

Fang, L.L., Wang, L.C., Chen, W.X., Sun, J., Cao, Q., Wang, S.Q., Wang, L.Z., 2021. Identifying the impacts of natural and human factors on ecosystem service in the yangtze and yellow river basins. J. Clean. Prod. 314 https://doi.org/10.1016/j.jclepro.2021.127995.

Fu, B.J., Wang, S., Su, C.H., Forsius, M., 2013. Linking ecosystem processes and ecosystem services. Curr. Opin. Environ. Sustain. 5 (1), 4–10. https://doi.org/10.1016/j.cosust.2012.12.002.

Garcia-Palacios, P., Gross, N., Gaitan, J., Maestre, F.T., 2018. Climate mediates the biodiversity-ecosystem stability relationship globally. Proc. Natl. Acad. Sci. u. s. a. 115 (33), 8400–8405. https://doi.org/10.1073/pnas.1800425115.

Ge, W.Y., Deng, L.Q., Wang, F., Han, J.Q., 2021. Quantifying the contributions of human activities and climate change to vegetation net primary productivity dynamics in china from 2001 to 2016. Sci. Total Environ. 773 https://doi.org/10.1016/j.scitotenv.2021.145648.

Gomes, L.C., Bianchi, F., Cardoso, I.M., Fernandes, E.I., Schulte, R., 2020. Land use change drives the spatio-temporal variation of ecosystem services and their interactions along an altitudinal gradient in brazil. Landsc. Ecol. 35 (7), 1571–1586. https://doi.org/10.1007/s10980-020-01037-1.

Gong, S., Xiao, Y., Zheng, H., Xiao, Y., Ouyang, Z., 2017. Spatial patterns of ecosystem water conservation in china and its impact factors analysis. Acta Ecologica Sinica 37 (7), 2455–2462.

Gonzalez-Garcia, A., Palomo, I., Gonzalez, J.A., Lopez, C.A., Montes, C., 2020. Quantifying spatial supply-demand mismatches in ecosystem services provides insights for land-use planning. Land Use Policy 94. https://doi.org/10.1016/j.landusepol.2020.104493.

Gret-Regamey, A., Altwegg, J., Siren, E.A., van Strien, M.J., Weibel, B., 2017. Integrating ecosystem services into spatial planning-a spatial decision support tool. Landsc. Urban Plan. 165, 206–219. https://doi.org/10.1016/j.landurbplan.2016.05.003.

Han, G.F., Xu, J.H., 2013. Land surface phenology and land surface temperature changes along an urban-rural gradient in yangtze river delta, china. Environ. Manage. 52 (1), 234–249. https://doi.org/10.1007/s00267-013-0097-6.

He, J.H., Pan, Z.Z., Liu, D.F., Guo, X.N., 2019. Exploring the regional differences of ecosystem health and its driving factors in china. Sci. Total Environ. 673, 553–564. https://doi.org/10.1016/j.scitotenv.2019.03.465.

Hernandez-Blanco, M., Costanza, R., Chen, H.J., Degroot, D., Jarvis, D., Kubiszewski, I., Montoya, J., Sangha, K., Stoeckl, N., Turner, K., Van'T Hoff, V., 2022. Ecosystem health, ecosystem services, and the well-being of humans and the rest of nature. Glob. Change Biol. 28 (17), 5027–5040. https://doi.org/10.1111/gcb.16281.

Hu, X., Hou, Y., Li, D., Hua, T., Marchi, M., Urrego, P.F.J., Huang, B., Zhao, W., Cherubini, F., 2023. Changes in multiple ecosystem services and their influencing factors in nordic countries. Ecol. Indic. 146, 109847 https://doi.org/10.1016/j.ecolind.2022.109847.

Hu, B., Kang, F., Han, H., Cheng, X., Li, Z., 2021. Exploring drivers of ecosystem services variation from a geospatial perspective: insights from china's shanxi province. Ecol. Indic. 131, 108188 https://doi.org/10.1016/j.ecolind.2021.108188.

Hu, C.G., Wang, Z.Y., Li, J.M., Liu, H., Sun, D.Q., 2022a. Quantifying the temporal and spatial patterns of ecosystem services and exploring the spatial differentiation of driving factors: a case study of sichuan basin, china. Front. Environ. Sci. 10 https://doi.org/10.3389/fenvs.2022.927818.

Hu, W., Yang, R., Jia, G., Yin, Z., Li, Y., Shen, S., Li, G., 2022c. Response of water yield function to land use change and its driving factors in the yangtze river basin. Acta Ecologica Sinica 42 (17), 7011–7027.

Hu, J., Zhang, J., Li, Y., 2022b. Exploring the spatial and temporal driving mechanisms of landscape patterns on habitat quality in a city undergoing rapid urbanization based on gtwr and mgwr: the case of nanjing, china. Ecol. Indic. 143, 109333 https://doi.org/10.1016/j.ecolind.2022.109333.

Huang, M., Fang, B., Yue, W., Feng, S., 2019. Spatial differentiation of ecosystem service values and its geographical detection in chaohu basin during 1995–2017. Geogr. Res. 38 (11), 2790–2803.

Huang, Y., Feng, T., Niu, S.F., Hao, D.S., Gan, X.Y., Zhou, B., 2022. Integrating the effects of driving forces on ecosystem services into ecological management: a case study from sichuan province, china. PLoS One 17 (6). https://doi.org/10.1371/journal.pone.0270365.

Kareiva, P., Tallis, H., Ricketts, T., Daily, G., Polasky, S., 2011. Natural capital: theory & practice of mapping ecosystem services. Oxford University Press, Oxford.

Khzr, B.O., Ibrahim, G., Hamid, A.A., Ail, S.A., 2022. Runoff estimation using scs-cn and gis techniques in the sulaymaniyah sub-basin of the kurdistan region of iraq. Environ. Dev. Sustain. 24 (2), 2640–2655. https://doi.org/10.1007/s10668-021-01549-z.

Kong, L.Q., Zheng, H., Rao, E.M., Xiao, Y., Ouyang, Z.Y., Li, C., 2018. Evaluating indirect and direct effects of eco-restoration policy on soil conservation service in yangtze river basin. Sci. Total Environ. 631–632, 887–894. https://doi.org/10.1016/j.scitotenv.2018.03.117.

Kreuter, U.P., Harris, H.G., Matlock, M.D., Lacey, R.E., 2001. Change in ecosystem service values in the san antonio area, texas. Ecol. Econ. 39 (3), 333–346. https://doi.org/10.1016/S0921-8009(01)00250-6.

Kroll, F., Muller, F., Haase, D., Fohrer, N., 2012. Rural-urban gradient analysis of ecosystem services supply and demand dynamics. Land Use Policy 29 (3), 521–535. https://doi.org/10.1016/j.landusepol.2011.07.008.

Li, J.H., 2022. Identification of ecosystem services supply and demand and driving factors in taihu lake basin. Environ. Sci. Pollut. Res. 29 (20), 29735–29745. https://doi.org/10.1007/s11356-021-17263-2.

Li, Z.Z., Hu, B.A., Qin, Y.Y., Cheng, X.Q., 2022c. Drivers of spatiotemporal disparities in the supply-demand budget of ecosystem services: a case study in the beijing-tianjin-hebei urban agglomeration, china. Front. Environ. Sci. 10 https://doi.org/10.3389/fenvs.2022.955876.

Li, T.N., Li, D.Z., Liang, D.L., Huang, S.M., 2022a. Coupling coordination degree of ecological-economic and its influencing factors in the counties of yangtze river economic belt. Sustainability 14 (22). https://doi.org/10.3390/su142215467.

Li, Y., Liu, W., Feng, Q., Zhu, M., Zhang, J., Yang, L., Yin, X., 2022b. Spatiotemporal dynamics and driving factors of ecosystem services value in the hexi regions, northwest china. Sustainability 14 (21), 14164. https://doi.org/10.3390/su142114164.

Li, F., Zhang, S.W., Yang, J.C., Bu, K., Wang, Q., Tang, J.M., Chang, L.P., 2016. The effects of population density changes on ecosystem services value: a case study in western jilin, china. Ecol. Indic. 61, 328–337. https://doi.org/10.1016/j.ecolind.2015.09.033.

Lin, H.W., Yun, H., 2023. Spatiotemporal dynamics of ecosystem services driven by human modification over the past seven decades: a case study of sihu agricultural watershed, china. Land 12, (3). https://doi.org/10.3390/land12030577.

Liu, J.G., Dietz, T., Carpenter, S.R., Alberti, M., Folke, C., Moran, E., Pell, A.N., Deadman, P., Kratz, T., Lubchenco, J., Ostrom, E., Ouyang, Z., Provencher, W., Redman, C.L., Schneider, S.H., Taylor, W.W., 2007. Complexity of coupled human and natural systems. Science 317 (5844), 1513–1516. https://doi.org/10.1126/science.1144004.

Liu, Y.B., Hou, X.Y., Li, X.W., Song, B.Y., Wang, C., 2020. Assessing and predicting changes in ecosystem service values based on land use/cover change in the bohai rim coastal zone. Ecol. Indic. 111 https://doi.org/10.1016/j.ecolind.2019.106004.

Liu, J., Wang, J., Dai, J., Zhai, T., Li, Z., 2021. The relationship between supply and demand of ecosystem services and its spatio-temporal variation in the yellow river basin. Journal of Natural Resources 36 (1), 148–161.

Liu, S.J., Wang, Z.J., Wu, W., Yu, L.F., 2022b. Effects of landscape pattern change on ecosystem services and its interactions in karst cities: a case study of guiyang city in china. Ecol. Indic. 145 https://doi.org/10.1016/j.ecolind.2022.109646.

Liu, H.Y., Xiao, W.F., Zhu, J.H., Zeng, L.X., Li, Q., 2022a. Urbanization intensifies the mismatch between the supply and demand of regional ecosystem services: a large-scale case of the yangtze river economic belt in china. Remote Sens. 14 (20) https://doi.org/10.3390/rs14205147.

Liu, W., Zhan, J.Y., Zhao, F., Wang, C., Zhang, F., Teng, Y.M., Chu, X., Kumi, M.A., 2022c. Spatio-temporal variations of ecosystem services and their drivers in the pearl river delta, china. J. Clean. Prod. 337 https://doi.org/10.1016/j.jclepro.2022.130466.

Ma, S., Qiao, Y.P., Wang, L.J., Zhang, J.C., 2021. Terrain gradient variations in ecosystem services of different vegetation types in mountainous regions: vegetation resource conservation and sustainable development. For. Ecol. Manage. 482 https://doi.org/10.1016/j.foreco.2020.118856.

Mu, X.L., Qiu, J.L., Cao, B.W., Cai, S.R., Niu, K.L., Yang, X.K., 2022. Mapping soil erosion dynamics (1990–2020) in the pearl river basin. Remote Sens. 14 (23) https://doi.org/10.3390/rs14235949.

Ni, R., Wang, F.E., Yu, J., 2022. Spatiotemporal changes in sustainable development and its driving force in the yangtze river delta region, china. J. Clean. Prod. 379 https://doi.org/10.1016/j.jclepro.2022.134751.

Pang, R.Q., Hu, N., Zhou, J.R., Sun, D.Q., Ye, H.Y., 2022. Study on eco-environmental effects of land-use transitions and their influencing factors in the central and southern liaoning urban agglomeration: a production-living-ecological perspective. Land 11 (6). https://doi.org/10.3390/land11060937.

Rao, E.M., Xiao, Y., Ouyang, Z.Y., Zheng, H., 2016. Changes in ecosystem service of soil conservation between 2000 and 2010 and its driving factors in southwestern china. Chin. Geogr. Sci. 26 (2), 165–173. https://doi.org/10.1007/s11769-015-0759-9.

Ren, B., Wang, Q., Zhang, R., Zhou, X., Wu, X., Zhang, Q., 2022. Assessment of ecosystem services: spatio-temporal analysis and the spatial response of influencing factors in hainan province. Sustainability 14 (15). https://doi.org/10.3390/su14159145.

Rial, J.A., Pielke, R.A., Beniston, M., Claussen, M., Canadell, J., Cox, P., Held, H., De Noblet-Ducoudre, N., Prinn, R., Reynolds, J.F., Salas, J.D., 2004. Nonlinearities, feedbacks and critical thresholds within the earth's climate system. Clim. Change 65 (1–2), 11–38. https://doi.org/10.1023/B:CLIM.0000037493.89489.3f.

Rong, Y.J., Li, K., Guo, J.W., Zheng, L.F., Luo, Y., Yan, Y., Wang, C.X., Zhao, C.L., Shang, X., Wang, Z.T., 2022. Multi-scale spatio-temporal analysis of soil conservation service based on mgwr model: a case of beijing-tianjin-hebei, china. Ecol. Indic. 139.

Rötzer, T., Rahman, M.A., Moser-Reischl, A., Pauleit, S., Pretzsch, H., 2019. Process based simulation of tree growth and ecosystem services of urban trees under present and future climate conditions. Sci. Total Environ. 676, 651–664. https://doi.org/10.1016/j.scitotenv.2019.04.235.

Sanchez-Canales, M., Benito, A.L., Passuello, A., Terrado, M., Ziv, G., Acuna, V., Schuhmacher, M., Elorza, F.J., 2012. Sensitivity analysis of ecosystem service valuation in a mediterranean watershed. Sci. Total Environ. 440, 140–153. https://doi.org/10.1016/j.scitotenv.2012.07.071.

Song, W., Deng, X.Z., 2017. Land-use/land-cover change and ecosystem service provision in china. Sci. Total Environ. 576, 705–719. https://doi.org/10.1016/j.scitotenv.2016.07.078.

Su, C., Fu, B., 2013. Evolution of ecosystem services in the chinese loess plateau under climatic and land use changes. Glob. Planet. Change 101, 119–128. https://doi.org/10.1016/j.gloplacha.2012.12.014.

Sun, L., Li, Z.J., Zhang, K., Jiang, T.T., 2021. Impacts of precipitation and topographic conditions on the model simulation in the north of china. Water Supply 21 (3), 1025–1035. https://doi.org/10.2166/ws.2020.284.

Sun, X., Tang, H.J., Yang, P., Hu, G., Liu, Z.H., Wu, J.G., 2020. Spatiotemporal patterns and drivers of ecosystem service supply and demand across the conterminous united states: a multiscale analysis. Sci. Total Environ. 703 https://doi.org/10.1016/j.scitotenv.2019.135005.

Sun, Q., Wang, C., Zhao, J., Zheng, J., Chen, J., 2011. Research evolution of rainfall erosivity(r)in china. Chinese Agricultural Science Bulletin 27 (4), 1–5.

Sun, B., Zhao, H., Lu, F., Wang, X., 2018. Spatial and temporal patterns of carbon sequestration in the northeastern forest regions and its impact factors analysis. Acta Ecologica Sinica 38 (14), 4975–4983.
Tan, F.F., Wang, F.Y., Niu, Z.Y., 2023. Multiscale disparity and spatial pattern of comprehensive carrying capacity in the yangtze river economic belt, china. Ecol. Indic. 148 https://doi.org/10.1016/j.ecolind.2023.110119.
Tang, Y.S., Tang, J.H., Yu, X.H., Qiu, L.F., Wang, J.Y., Hou, X.R., Chen, D.X., 2022. Land ecological protection polices improve ecosystem services: a case study of lishui, china. Front. Environ. Sci. 10 https://doi.org/10.3389/fenvs.2022.973524.
Tang, D.C., Zhang, Y., Bethel, B.J., 2019. An analysis of disparities and driving factors of carbon emissions in the yangtze river economic belt. Sustainability 11 (8). https://doi.org/10.3390/su11082362.
Tedesco, A.M., Brancalion, P., Hepburn, M., Walji, K., Wilson, K.A., Possingham, H.P., Dean, A.J., Nugent, N., Elias-Trostmann, K., Perez-Hammerle, K.V., Rhodes, J.R., 2023. The role of incentive mechanisms in promoting forest restoration. Philos. Trans. R. Soc. B-Biol. Sci. 378 (1867). https://doi.org/10.1098/rstb.2021.0088.
The State Council Information Office of the People's Republic of China, 2020. The state council of the people's republic of china has published english translations of 61 commonly used keywords of major national strategies. accessed 2023-12-26. http://www.scio.gov.cn/zdgz/gzdt1/202308/t20230816_750811.html.
Tian, H.L., Zhu, J.H., Jian, Z.J., Ou, Q.X., He, X., Chen, X.Y., Li, C.Y., Li, Q., Liu, H.Y., Huang, G.S., Xiao, W.F., 2022. The carbon neutral potential of forests in the yangtze river economic belt of china. Forests 13 (5). https://doi.org/10.3390/f13050721.
Tong, X.W., Wang, K.L., Brandt, M., Yue, Y.M., Liao, C.J., Fensholt, R., 2016. Assessing future vegetation trends and restoration prospects in the karst regions of southwest china. Remote Sens. 8 (5) https://doi.org/10.3390/rs8050357.
Tu, A.G., Xie, S.H., Yu, Z.B., Li, Y., Nie, X.F., 2018. Long-term effect of soil and water conservation measures on runoff, sediment and their relationship in an orchard on sloping red soil of southern china. PLoS One 13 (9). https://doi.org/10.1371/journal.pone.0203669.
Venables, W.N., Ripley, B.D., 2002. Modern applied statistics with s. Springer.
Wang, Y.Z., Zou, H., Duan, X.J., Wang, L.Q., 2022. Coordinated evolution and influencing factors of population and economy in the yangtze river economic belt. INTERNATIONAL JOURNAL OF ENVIRONMENTAL RESEARCH AND PUBLIC HEALTH 19 (21). https://doi.org/10.3390/ijerph192114395.
Wang, L.J., Ma, S., Jiang, J., Zhao, Y.G., Zhang, J.C., 2021. Spatiotemporal variation in ecosystem services and their drivers among different landscape heterogeneity units and terrain gradients in the southern hill and mountain belt, china. Remote Sens. 13 (7) https://doi.org/10.3390/rs13071375.
Wang, L.J., Gong, J.W., Ma, S., Wu, S., Zhang, X.M., Jiang, J., 2022a. Ecosystem service supply-demand and socioecological drivers at different spatial scales in zhejiang province, china. Ecol. Indic. 140 https://doi.org/10.1016/j.ecolind.2022.109058.
Wang, Z.M., Li, Q.Z., Liu, L., Zhao, H.L., Ru, H.E., Wu, J.P., Deng, Y.L., 2023c. Spatiotemporal evolution and attribution analysis of water yield in the xiangjiang river basin (xrb) based on the invest model. Water 15, (3). https://doi.org/10.3390/w15030514.
Wang, D., Tian, Y., Zhang, Y., Huang, L., Tao, J., Yang, Y., Lin, J., Zhang, Q., 2023. Evaluation and quantitative attribution analysis of water yield services in the peak-cluster depression basins in southwest of guangxi, china. Chin. Geogr. Sci. 33 (1), 116–130. https://doi.org/10.1007/s11769-023-1329-1.
Wang, Y.X., Wang, H.M., Liu, G., Zhang, J.X., Fang, Z., 2022c. Factors driving water yield ecosystem services in the yellow river economic belt, china: spatial heterogeneity and spatial spillover perspectives. J. Environ. Manage. 317 https://doi.org/10.1016/j.jenvman.2022.115477.
Wang, X.Z., Wu, J.Z., Liu, Y.L., Hai, X.Y., Shanguan, Z.P., Deng, L., 2022b. Driving factors of ecosystem services and their spatiotemporal change assessment based on land use types in the loess plateau. J. Environ. Manage. 311 https://doi.org/10.1016/j.jenvman.2022.114835.
Wehrens, R., Kruisselbrink, J., 2018. Flexible self-organizing maps in kohonen 3.0. J. Stat. Softw. 87 (7), 1–18. https://doi.org/10.18637/iss.v087.i07.
Wei, P., Wu, M., Jia, Y., Gao, Y., Xu, H., Liu, Z., Chen, S., 2022. Spatiotemporal variation of water yield in the upstream regions of the shule river basin using the invest model. Acta Ecologica Sinica 42 (15), 6418–6429.
Williams, J.R., Jones, C.A., Kiniry, J.R., Spanel, D.A., 1989. The epic crop growth-model. TRANSACTIONS OF THE ASAE 32 (2), 497–511.
Wu, J.S., Fan, X.N., Li, K.Y., Wu, Y.W., 2023. Assessment of ecosystem service flow and optimization of spatial pattern of supply and demand matching in pearl river delta, china. Ecol. Indic. 153 https://doi.org/10.1016/j.ecolind.2023.110452.
Wu, C.X., Qiu, D.X., Gao, P., Mu, X.M., Zhao, G.J., 2022a. Application of the invest model for assessing water yield and its response to precipitation and land use in the weihe river basin, china. J. Arid Land 14 (4), 426–440. https://doi.org/10.1007/s40333-022-0013-0.
Wu, D., Zou, C., Cao, W., Liu, L., 2018. Analysis of the ecosystem soil conservation function based on the major function-oriented zones across the yangtze river economic belt, china. Sustainability 10 (10), 3425. https://doi.org/10.3390/su10103425.
Wu, D., Zou, C.X., Lin, N.F., Xu, M.J., 2021. Tradeoffs and synergies among ecosystem services in the yangtze river economic belt, china. Environmental Ecology 3 (09), 1–7.
Xiang, H.L., Yang, J., Liu, X., Lee, J., 2019. Balancing population distribution and sustainable economic development in yangtze river economic belt of china. Sustainability 11 (12). https://doi.org/10.3390/su11123320.
Xiao, Q., Hu, D., Xiao, Y., 2017. Assessing changes in soil conservation ecosystem services and causal factors in the three gorges reservoir region of china. J. Clean. Prod. 163, S172–S180. https://doi.org/10.1016/j.jclepro.2016.09.012.
Xiao, Y., Ouyang, Z.Y., 2019. Spatial-temporal patterns and driving forces of water retention service in china. Chin. Geogr. Sci. 29 (1), 100–111. https://doi.org/10.1007/s11769-018-0984-0.
Xie, G., Zhang, C., Zhang, C., Xiao, Y., Lu, C., 2015. The value of ecosystem services in china. Resources Science 37 (9), 1740–1746.
Xu, X.B., Yang, G.S., Tan, Y., Liu, J.P., Hu, H.Z., 2018. Ecosystem services trade-offs and determinants in china's yangtze river economic belt from 2000 to 2015. Sci. Total Environ. 634, 1601–1614. https://doi.org/10.1016/j.scitotenv.2018.04.046.
Xue, C.L., Chen, X.H., Xue, L.R., Zhang, H.Q., Chen, J.P., Li, D.D., 2023. Modeling the spatially heterogeneous relationships between tradeoffs and synergies among ecosystem services and potential drivers considering geographic scale in bairin left banner, china. Sci. Total Environ. 855 https://doi.org/10.1016/j.scitotenv.2022.158834.
Yan, Y.J., Dai, Q.H., Yuan, Y.F., Peng, X.D., Zhao, L.S., Yang, J., 2018. Effects of rainfall intensity on runoff and sediment yields on bare slopes in a karst area, sw china. Geoderma 330, 30–40. https://doi.org/10.1016/j.geoderma.2018.05.026.
Yang, M.H., Gao, X.D., Zhao, X.N., Wu, P.T., 2021. Scale effect and spatially explicit drivers of interactions between ecosystem services-a case study from the loess plateau. Sci. Total Environ. 785 https://doi.org/10.1016/j.scitotenv.2021.147389.
Yang, Y.Q., Jun, Z., Sui, X., He, X., 2020. Study of the spatial connection between urbanization and the ecosystem-a case study of central yunnan (china). PLoS One 15 (9). https://doi.org/10.1371/journal.pone.0238192.
Ye, X., Wang, Y., Pan, H., Bai, Y., Dong, D., Yao, H., 2022. Spatial-temporal variation and driving factors of vegetation net ecosystem productivity in qinghai province. Arid Zone Research 39 (5), 1673–1683.
Yin, G., Wang, X., Zhang, X., Fu, Y., Hao, F., Hu, Q., 2020. Invest model-based estimation of water yield in north china and its sensitivities to climate variables. Water 12 (6). https://doi.org/10.3390/w12061692.
Yuan, L., Li, R.Y., He, W.J., Wu, X., Kong, Y., Degefu, D.M., Ramsey, T.S., 2022. Coordination of the industrial-ecological economy in the yangtze river economic belt, china. Front. Environ. Sci. 10 https://doi.org/10.3389/fenvs.2022.882221.
Zhang, L., Dawes, W.R., Walker, G.R., 2001. Response of mean annual evapotranspiration to vegetation changes at catchment scale. Water Resour. Res. 37 (3), 701–708. https://doi.org/10.1029/2000WR900325.
Zhang, L.G., Hu, N.K., 2021. Spatial variation and terrain gradient effect of ecosystem services in heihe river basin over the past 20 years. Sustainability 13 (20). https://doi.org/10.3390/su132011271.
Zhang, J., Shi, Y., Xian, C.F., Zhang, L., Zou, Z.Y., 2022. How urbanization affect the ecosystem health of tibet based on terrain gradients: a case study of shannan, china. Ecosyst. Health Sustain. 8 (1) https://doi.org/10.1080/20964129.2022.2097449.
Zhang, M.Y., Wang, K.L., Liu, H.Y., Zhang, C.H., Yue, Y.M., Qi, X.K., 2018. Effect of ecological engineering projects on ecosystem services in a karst region: a case study of northwest guangxi, china. J. Clean. Prod. 183, 831–842. https://doi.org/10.1016/j.jclepro.2018.02.102.
Zhang, Y.X., Wang, Y.K., Fu, B., Dixit, A.M., Chaudhary, S., Wang, S., 2020. Impact of climatic factors on vegetation dynamics in the upper yangtze river basin in china. J Mt. Sci. 17 (5), 1235–1250. https://doi.org/10.1007/s11629-019-5649-7.
Zhang, W., Xie, Y., Liu, B., 2002. Rainfall erosivity estimation using daily rainfall amounts. Scientia Geographica Sinica 22 (6), 705–711.
Zhao, J.Y., Li, J.J., Zuo, L.L., Liu, G.H., Su, X.K., 2023. Interaction dynamics of multiple ecosystem services and abrupt changes of landscape patterns linked with watershed ecosystem regime shifts. Ecol. Indic. 150 https://doi.org/10.1016/j.ecolind.2023.110263.
Zhao, Z., Zhang, Y., Pan, Y., Wu, J., Li, Z., 2020. Changes in human activity intensity and influence on ecosystem regulating services: a study of tibet based on night light data. Journal of Geo-Information Science 22 (7), 1544–1554.
Zhao, J., Zhao, Y.L., 2023. Synergy/trade-offs and differential optimization of production, living, and ecological functions in the yangtze river economic belt, china. Ecol. Indic. 147 https://doi.org/10.1016/j.ecolind.2023.109925.
Zhu, K., Zhou, Q., Cheng, Y.F., Zhang, Y.T., Li, T., Yan, X.Y., Alimov, A., Farmanov, E., David, L.D., 2023. Regional sustainability: pressures and responses of tourism economy and ecological environment in the yangtze river basin, china. Front. Ecol. Evol. 11 https://doi.org/10.3389/fevo.2023.1148868.

Further reading

Wu, J.H., Wang, G.Z., Chen, W.X., Pan, S.P., Zeng, J., 2022b. Terrain gradient variations in the ecosystem services value of the qinghai-tibet plateau, china. Glob. Ecol. Conserv. 34 https://doi.org/10.1016/j.gecco.2022.e02008.